The Journal of Experimental Biology 209, 789-800
Published by The Company of Biologists 2006
doi:10.1242/jeb.02053

Crepuscular and nocturnal illumination and its effects on color perception by the nocturnal hawkmoth *Deilephila elpenor*

Sönke Johnsen[1,*], Almut Kelber[2], Eric Warrant[2], Alison M. Sweeney[1], Edith A. Widder[3], Raymond L. Lee, Jr[4] and Javier Hernández-Andrés[5]

[1]*Biology Department, Duke University, Durham, NC 27708, USA,* [2]*Department of Cell and Organism Biology, Lund University, Sweden,* [3]*Marine Science Division, Harbor Branch Oceanographic Institution, Fort Pierce, FL 34946, USA,* [4]*Mathematics and Science Division, US Naval Academy, Annapolis, MD 21402, USA and* [5]*Optics Department, University of Granada, Spain*

*Author for correspondence (e-mail: sjohnsen@duke.edu)

Accepted 20 December 2005

Summary

Recent studies have shown that certain nocturnal insect and vertebrate species have true color vision under nocturnal illumination. Thus, their vision is potentially affected by changes in the spectral quality of twilight and nocturnal illumination, due to the presence or absence of the moon, artificial light pollution and other factors. We investigated this in the following manner. First we measured the spectral irradiance (from 300 to 700 nm) during the day, sunset, twilight, full moon, new moon, and in the presence of high levels of light pollution. The spectra were then converted to both human-based chromaticities and to relative quantum catches for the nocturnal hawkmoth *Deilephila elpenor*, which has color vision. The reflectance spectra of various flowers and leaves and the red hindwings of *D. elpenor* were also converted to chromaticities and relative quantum catches. Finally, the achromatic and chromatic contrasts (with and without von Kries color constancy) of the flowers and hindwings against a leaf background were determined under the various lighting environments. The twilight and nocturnal illuminants were substantially different from each other, resulting in significantly different contrasts. The addition of von Kries color constancy significantly reduced the effect of changing illuminants on chromatic contrast, suggesting that, even in this light-limited environment, the ability of color vision to provide reliable signals under changing illuminants may offset the concurrent threefold decrease in sensitivity and spatial resolution. Given this, color vision may be more common in crepuscular and nocturnal species than previously considered.

Key words: hawkmoth, *Deilephila elpenor*, nocturnal vision, color vision, environmental optics.

Introduction

While multiple visual pigments in certain deep-sea species (Cronin and Frank, 1996; Douglas et al., 1998) and multiple rod types in amphibians (Makino-Tasaka and Suzuki, 1984) have been known for some time, unambiguous evidence for true color vision under scotopic conditions has only recently been acquired (Kelber et al., 2002; Roth and Kelber, 2004). These behavioral studies, which show that the nocturnal hawkmoth *Deilephila elpenor* and the nocturnal helmet gecko *Tarentola chazaliae* can discern color under starlight and dim moonlight, respectively, raise at least two issues.

First, what is the selective advantage of color vision in these species that outweighs its costs? Color vision's detrimental effect on spatial resolution and the additional structural and neurological complexity required for color processing makes it a more difficult proposition for all species. However, color vision presents additional difficulties for nocturnal species. While the decrease in sensitivity associated with the increase in the number of visual channels has little effect on species operating during light-saturated diurnal conditions, this sensitivity loss can potentially affect the ability of nocturnal species to function in their light-limited environment. It is primarily for this reason that color vision has generally been expected to be rare or absent among nocturnal species (Jacobs, 1993).

Second, what color are objects when viewed under the night sky? Although not perceived by humans, the spectrum of the night sky is not neutral, and depends on multiple factors, including how far the sun is below the horizon, the presence or absence and phase of the moon and, recently, on the level of light pollution (e.g. Munz and McFarland, 1977; Endler, 1991; Leinert et al., 1998; McFarland et al., 1999; Cinzano et al., 2001; Hernández-Andrés et al., 2001; Lee and Hernández-

Andrés, 2003). It has long been known that the variation of daytime spectra, due to cloud cover, solar elevation, forest canopy and depth (for aquatic species), has a substantial effect on the appearance and visibility of objects and organisms, which can be at least partly ameliorated by color vision (Wyszecki and Stiles, 1982; Endler, 1991; McFarland et al., 1999; Johnsen and Sosik, 2003; Lovell et al., 2005). Less work, however, has been done on the appearance of objects during twilight (reviewed by McFarland et al., 1999; Rickel and Genin, 2005), and, to our knowledge, the appearance of objects under different nocturnal illuminants has received very little attention.

This study measures or models spectral irradiance (300–700 nm) during daylight, sunset, twilight, moonlit nights, moonless nights and nights in regions with high light pollution. These spectra, in addition to previously published data, are then used to calculate the relative quantum catches of the three photoreceptors of *D. elpenor* under different lighting conditions. In addition to the general illuminants, relative quantum catches of five stimuli (green leaves, three flowers and the red hindwing of *D. elpenor*) are also calculated. Three different types of contrasts of the latter four stimuli viewed against green leaves are then determined: (1) achromatic contrast, (2) chromatic contrast and (3) chromatic contrast assuming von Kries color constancy. Finally, quantum catches of hypothetical photoreceptors with varying wavelengths of peak absorption are compared to the catches of the long wavelength receptor in *D. elpenor* under the different illuminants.

Materials and methods

General approach

The goal of this study was to determine the range of spectra found during sunset, twilight and night. Therefore, rather than measure a large number of spectra under all possible celestial and atmospheric conditions, we measured spectra under various extreme conditions. Both human-based chromaticities and the relative quantum catches described below have the property that the value of the mixture of two illuminants falls between the values of the two illuminants alone (Wyszecki and Stiles, 1982). Thus, by measuring the spectra under conditions where one of the various contributors to the illumination dominates, we can define the boundaries of the region where most spectra are found. The following four conditions were thus of particular interest: (1) clear nautical twilight (solar elevation between –6° and –12°), (2) full moon at high elevation under clear skies, (3) moonless and clear night and (4) urban overcast and moonless sky. The irradiances under these conditions correspond to nearly complete dominance by the following four factors respectively: (1) scattered sunlight modified by ozone absorption, (2) moonlight, (3) starlight and (4) anthropogenic illumination. These spectra were then compared with 2600 spectra of daylight, sunset and civil twilight (solar elevation between 0° and –6°) and 220 spectra of daylight under a forest canopy using a model of color vision for the nocturnal hawkmoth, *Deilephila elpenor* L.

Measurement of twilight spectra

Fourteen sunset and twilight measurements of spectral irradiance under minimal cloud cover were taken on the beaches of two barrier islands located off the coast of North Carolina, USA (Atlantic Beach; 34°42′N 76°44′W and Cape Hatteras National Seashore; 35°44′N 75°32′W, both at sea level) on 11 June, 12 June and 17 July, 2004. The locations were chosen to maximize the view of the sky and minimize the effects of anthropogenic light. Spectra were taken using a USB2000 spectrometer (Ocean Optics Inc., Dunedin, FL, USA) that had been modified for increased sensitivity by increasing the width of the entrance slit to 200 μm and focusing light onto the detector array with a collector lens (L2 collector lens, Ocean Optics). The spectrometer was fitted with a 1 mm diameter fiber optic cable that viewed a horizontal slab of a Lambertian reflector (Spectralon, Labsphere Inc., North Sutton, NH, USA). Because Lambertian materials reflect light evenly in all directions, their radiance is proportional to the irradiance striking them (Palmer, 1995). This method of obtaining the cosine response needed for measuring diffuse irradiance was chosen because it is more efficient than the typical diffusely transmitting disk (Doxaran et al., 2004).

Spectra were taken at solar elevations ranging from +11° to –11° (elevations determined using tables from the United States Naval Observatory). At lower solar elevations, the integration time of the spectrometer was increased to a maximum of 10 s, with 30 such integrations averaged per measurement. Spectra were taken from 300 to 700 nm and averaged over 5 nm intervals.

Measurement of full moonlight and synthesis of starlight spectra

Spectral irradiance under the full moon was measured using a spectrometer with a highly sensitive photomultiplier detector (OL-754-PMT, Optronics Laboratories Inc., Orlando, FL, USA). Spectra were taken on 10 December, 2003 at Harbor Branch Oceanographic Institution (Fort Pierce, FL, USA; 27°26′N 80°19′W, sea level) during the full moon (elevation 69°, moon 98% full). An integrating sphere was used to ensure a cosine angular response. Data were taken at 5 nm intervals from 350 to 700 nm.

Preliminary attempts showed that even the OL-754 spectrometer was not sensitive enough to measure spectral irradiance on a moonless night. Therefore it was calculated in the following manner. The spectral radiances of small star-free portions of the moonless night sky were obtained from two observatories: Kitt Peak National Observatory (Tuscon, AZ, USA; 31°58′N 111°36′W, elevation 2083 m) and the William Herschel Telescope (La Palma, Canary Islands, Spain; 28°36′N 17°45′W, elevation 2400 m) (Benn and Ellison, 1998; Massey and Foltz, 2000). Star and moon-free night spectra are composed primarily of airglow (emission spectra of the various molecular components of the upper atmosphere)

and zodiacal light (sunlight scattered from the dust in the plane of the solar system) (Leinert et al., 1997; Benn and Ellison, 1998). Because airglow is relatively constant over the entire hemisphere and zodiacal light is concentrated in a small region near the horizon, the former is the primary contributor to the diffuse irradiance of a star-free night sky (~80%) (Benn and Ellison, 1998). The stars contribute approximately 23–33% of the total irradiance, depending on the solar activity level (which affects the airglow intensity). The average spectrum of the stars of all spectral types (weighted by their relative abundances) was taken from Matilla (1980). This spectrum was combined with the star-free night sky spectra and integrated over the entire hemisphere of the sky to obtain estimates of the spectral irradiance on moonless nights. Two spectra were calculated from each observatory spectrum, one for the solar minimum (when stars contribute 33% of the total irradiance) and one for the solar maximum, (when stars contribute 23%). Spectra were calculated at 5 nm intervals from 300 to 700 nm.

To determine the effect of anthropogenic light on nocturnal irradiance, a spectrum was obtained from an urban location on a cloudy night (Jamaica Pond, Boston, MA, USA, 42°20′N 71°03′W, sea level) (M. Moore, unpublished data). Cloudy conditions were chosen because they maximize the effects of light pollution by reflecting urban lighting back to the ground. The measurement technique and resolution matched that described above for the North Carolina twilight spectra.

Daylight, civil twilight, and forest spectra

An estimate of the variability of daylight and civil twilight spectra (to compare with the variability during twilight and night) was obtained from 2395 daylight, 254 civil twilight and 220 forest measurements of spectral irradiance (Chiao et al., 2000; Hernández-Andrés et al., 2001; Lee and Hernández-Andrés, 2003). All the daylight and 205 of the civil twilight spectra were measured from the roof of the University of Granada's Science Faculty (Granada, Spain, 37°11′N 3°35′W, elevation 680 m) from February 1996 to February 1998 using a LI-1800 spectroradiometer (LI-COR Bioscience, Lincoln, NE, USA) fitted with a cosine-corrected receptor. Measurements were taken at all solar elevations greater than –4° and in all weather except for rain or snowfall. Data were collected at 5 nm intervals from 300 to 1100 nm. Another 49 civil twilight spectra were measured from three sites: Owings, MA, USA (38°41′N 76°35′W, elevation 15 m), Annapolis, MA, USA (38°59′N 76°29′W, elevation 18 m), and Marion Center, PA, USA (40°49′N 79°05′W, elevation 451 m). Measurements (from 380–780 nm) were taken from 1998 to 2001 using PR-650 spectroradiometer (Photo Research Inc., Chatsworth, CA, USA). Solar elevation ranged from 0° to –5.6°.

The 220 forest spectra were measured from sunrise to sunset during July and August 1999 in several temperate forests in Maryland, USA. Measurement locations included both full shade and under gaps in the canopy, and atmospheric conditions ranged from clear to overcast. Data were collected at 3 nm intervals from 400 to 700 nm using an S2000 spectroradiometer (Ocean Optics) fitted with a cosine corrector.

UV and visible reflectance curves

The spectral reflectance of the white flower of the hawkmoth-pollinated evening primrose *Oenothera neomexicana* Munz (Raguso and Willis, 2002) and of the blue flower of the unspotted lungwort *Pulmonaria obscura* L. and the yellow flower of the birdsfoot trefoil *Lotus corniculatus* L.(Chittka et al., 1994) were used and are typical for white, yellow and blue flowers, respectively (although the flowers of certain species have higher reflectance at UV wavelengths). Reflections from a green leaf and the red area on the wings of the nocturnal hawkmoth *Deilephila elpenor* were measured using an S2000 Spectrometer (Ocean Optics) calibrated with a diffuse reflectance standard (WS1, Ocean Optics). All five spectra are shown in Fig. 1A.

Receptor sensitivities and photon catch calculation

The number of photons N that are absorbed by the

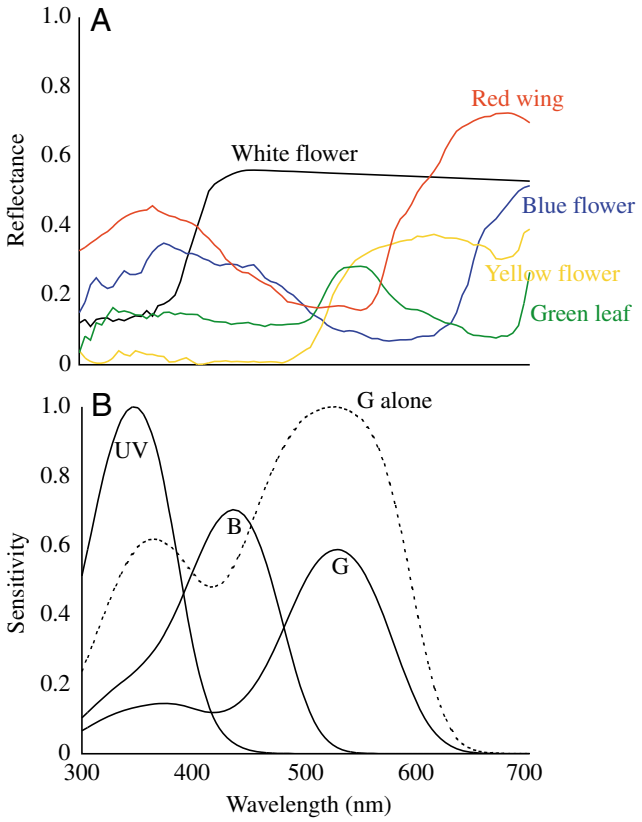

Fig. 1. (A) Spectral reflectance of stimuli (1=100%). (B) Spectral sensitivities of the photoreceptors of *Deilephila elpenor* assuming fused rhabdoms containing all three photoreceptor types. UV, B and G refer to the photoreceptors with peak absorption wavelengths of 350, 440, and 525 nm, respectively. Solid lines show normalized receptor sensitivities that were used to calculate relative quantum catches. The broken line shows the sensitivity of the green receptor that was used for the achromatic contrast calculations.

photoreceptors in one ommatidium of the nocturnal hawkmoth, *Deilephila elpenor*, per integration time of the photoreceptor, is given by:

$$N = 1.13\left(\frac{\pi}{4}\right) n\Delta\rho^2 D^2 \Delta t \int \kappa\tau(1-e^{-kR_i(\lambda)l})L(\lambda)d\lambda \qquad (1)$$

(Warrant and Nilsson, 1998; Kelber et al., 2002; Kelber et al., 2003a; Warrant, 2004). $L(\lambda)$ is the stimulus radiance in photons m^{-2} s^{-1} nm^{-1} sr^{-1}. $R_i(\lambda)$ (i=1,2,3) are the absorbance spectra of the three visual pigments of *D. elpenor*, calculated from their recorded sensitivity maxima (350 nm, 440 nm and 525 nm) (Schwemer and Paulsen, 1973; Höglund et al., 1973) using the Stavenga–Smits–Hoenders rhodopsin template (Stavenga et al., 1993) and equations 2a and 2b (Snyder et al., 1973). The other variables are given in Table 1.

For the calculation of the relative quantum catches, we assumed that the eyes of *D. elpenor* have fused rhabdoms with all three receptor types. This is a simplification because it is likely that there are two additional ommatidial types, one with blue and green receptors only, and one with UV and green receptors only (Kelber et al., 2002). However, because it is not known whether and how color processing involves inter-ommatidial connections, the ommatidial type containing all three receptors was the most general to model. Quantum catches were calculated assuming lateral screening (Snyder et al., 1973) (see Appendix for complete derivation). The receptor sensitivities were all normalized so that their integrals equalled 1. Thus, a stimulus that induces the same response in each photoreceptor type has its color locus in the centre of the color triangle (for details, see Kelber et al., 2003b).

Independent receptor adaptation was used as a model of chromatic adaptation (von Kries, 1904; Kelber et al., 2003b). This assumes that receptors adapt to the background intensity by keeping the response at approximately 50% of their maximal response (Laughlin and Hardie, 1978). The adapted receptor signal q is then:

$$q = N/N_b\,, \qquad (2)$$

where N is quantum catch of a receptor viewing the stimulus and N_b is the quantum catch of the same receptor viewing the background. The radiance of the green leaves under the different illuminants was used as the background.

Table 1. *Optical and visual parameters for Deilephila elpenor*

Parameter	Description	Value
n	Effective facets in the superposition aperture	568
$\Delta\rho$	Photoreceptor acceptance angle	3.0°
D	Diameter of a facet lens	29 μm
κ	Quantum efficiency of transduction	0.5
τ	Fractional transmission of the eye media	0.8
Δt	Integration time of a photoreceptor	0.036 s
k	Absorption coefficient of the rhabdom	0.0067 μm^{-1}
l	Rhabdom length, doubled by tapetal reflection	414 μm

For calculating achromatic contrast, we assumed that green receptors extend over the entire length and width of the rhabdom and no lateral screening takes place (Fig. 1B, broken line). The achromatic contrast C was then calculated as:

$$C = \frac{N_x - N_{green}}{N_x + N_{green}}\,, \qquad (3)$$

where N_x is the number of absorbed photons from the colored foreground and N_{green} is the number of absorbed photons from the green leaf background.

Because the spectra of nocturnal illumination are generally long-shifted (see Results), the 525 nm green pigment of *D. elpenor* may not be efficient at capturing this light. This possibility was examined by calculating the absolute photon catch of the long-wavelength pigment as a function of its peak wavelength. As was done for the achromatic contrast calculations, we assumed that green receptors extended over the entire length and width of the rhabdom and no lateral screening took place.

Results

Sunset, twilight and nocturnal spectra

Spectral irradiance changed substantially during sunset and twilight (Fig. 2A,B). As solar elevation decreased from 10° to 0°, the illumination gradually changed from being long-wavelength shifted to relatively spectrally neutral. After the disappearance of the sun's disk (thick line in Fig. 2A shows sunset), the spectra were dominated by a broad peak centered at ~450 nm, which became increasingly prominent as twilight progressed.

Nocturnal spectral irradiance was strongly affected by the presence or absence of the moon. Under a full moon at 70° elevation, the spectrum was nearly indistinguishable from a typical daylight spectrum. In the absence of the moon, the spectrum was shifted to longer wavelengths and displayed four narrow, but prominent peaks (at 560, 590, 630 and 685 nm). A moonless sky in a region with high amounts of light pollution was substantially long-wavelength shifted, with a broad peak centered at 590 nm.

Human-based chromaticity and relative quantum catches in D. elpenor

Mapping the twilight and nocturnal spectra into the perceptually uniform, human-based u′v′ chromaticity space showed that nautical twilight (solar elevation between –6° and –12°), moonless nights, and regions with high light pollution, had chromaticities well outside the envelope of those of the daylight, forest and early twilight illuminants (Fig. 3A). The same was also true for the relative quantum catches of *D. elpenor*, although the relative positions of starlight *vs* daylight *vs* twilight were different (Fig. 3B). The illumination of the full moon mapped to the long-wavelength border of the Granada daylight coordinates in both color spaces.

If humans had nocturnal color vision, these spectral shifts

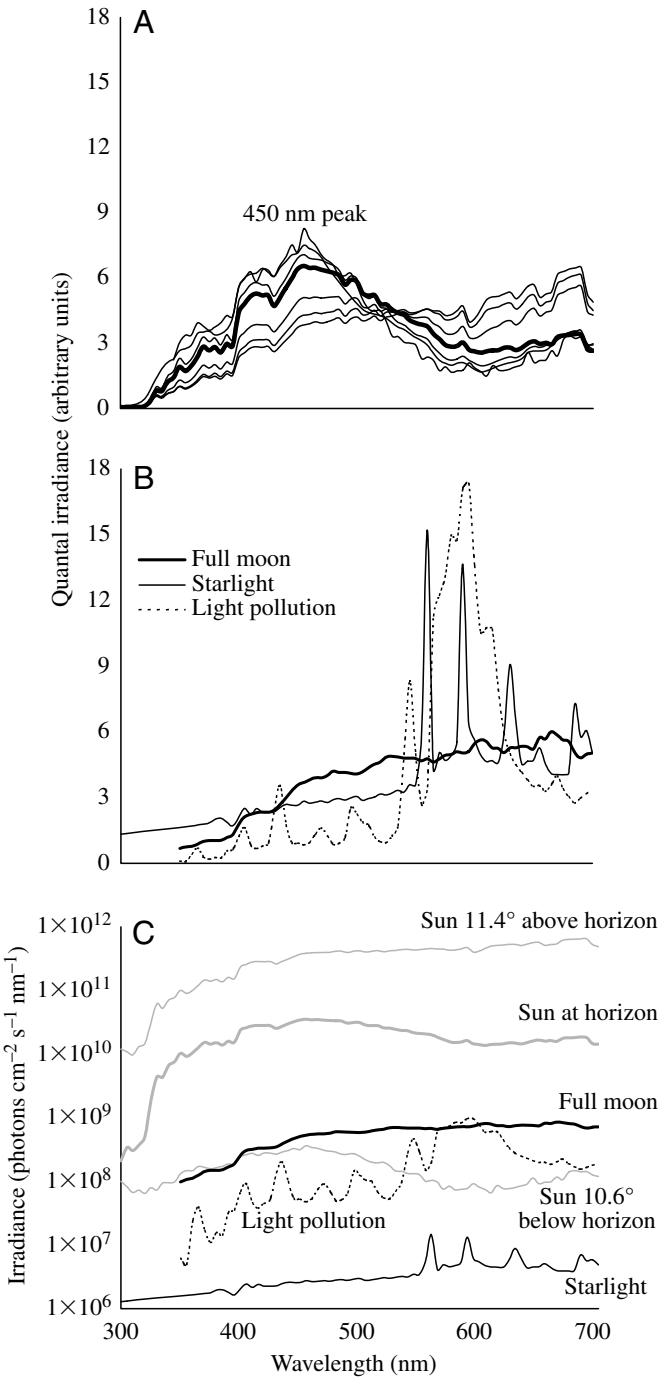

Fig. 2. (A) Normalized quantal irradiance during sunset and twilight. The thick line denotes a spectrum taken at sunset (solar elevation –0.6°). The three lines with long-wavelength irradiance greater than at sunset denote solar elevations of 11°, 5.9° and 1.0° (in order of decreasing long-wavelength values). The three lines with 450 nm peak values greater than at sunset denote solar elevations of –3.6°, –6.5° and –9.3° (in order of increasing 450 nm peak values). (B) Normalized quantal irradiance due to three common sources of nocturnal illumination. Spectra in A and B are normalized so that their irradiances integrated from 350 to 700 nm are all equal. (C) Unnormalized spectra. All spectra presented in this study, with the exception of those taken within forests, are freely available from the authors.

would be quite noticeable. When viewed under a light-polluted night, the evening primrose *Oenothera neomexicana* would appear far redder than under daylight. The same red shift, though smaller, would also be observed under starlight. When viewed under nautical twilight, the view would be strongly blue-shifted.

Relative quantum catches of flowers, leaves and wings

The relative quantum catches of the five examined stimuli (blue, white and yellow flowers; green leaves; red hindwings of *D. elpenor*) depended strongly on the source of illumination (Fig. 4A,B). In general, the variation was primarily in the relative quantum catch of the green photoreceptor (i.e. along a line connecting the green vertex to the UV–blue side). Decreasing solar elevation lowered the relative catch of the green receptor, with a slight increase in the relative catch of the UV receptor in nautical twilight. The type of nocturnal illumination affected the relative quantum catches to a similar degree, with all three illuminants (moonlight, starlight, light pollution) resulting in higher relative quantum catches in the green receptor. In general, the stimuli viewed under light-polluted skies had relative quantum catches substantially different from those under all natural illuminants, both crepuscular and nocturnal.

The variation of relative quantum catch was roughly similar among the five stimuli. The smallest and largest variations under twilight were found in the blue flower and green leaf stimuli respectively (Fig. 4B). The smallest and largest variations under the three nocturnal illuminants were found in the yellow flower and red wing stimuli respectively (Fig. 4A,B).

When von Kries color constancy was assumed, the variation of all five stimuli under the various illuminants was substantially less (Fig. 4C). The largest variation was found in the blue and yellow flower stimuli. The smallest variation was found in the red wing stimulus.

Achromatic and chromatic contrasts

The variation in achromatic contrast of the stimuli against the leaves under twilight, moonlight and starlight was strongly dependent on the stimulus (Fig. 5A,D). The achromatic contrast of the white flower stimulus was fairly independent of illuminant, with a coefficient of variation (i.e. standard deviation divided by the mean) of about 5%. In contrast, the achromatic contrasts of the yellow and blue flower stimuli had coefficients of variation higher than 100%. In addition, under full moon and starlight, their achromatic contrasts against the leaf were nearly zero. When the contrast of the two flowers under light polluted skies were also considered, the variation was even larger, with the contrasts switching polarities. The coefficient of variation of the red wing against the green leaves had an intermediate value of 27%.

In the case of chromatic contrasts (estimated as the distance between the relative quantum catches of the stimuli and the leaf background), the variation was in general lower and less dependent on stimulus, with coefficients of variation ranging

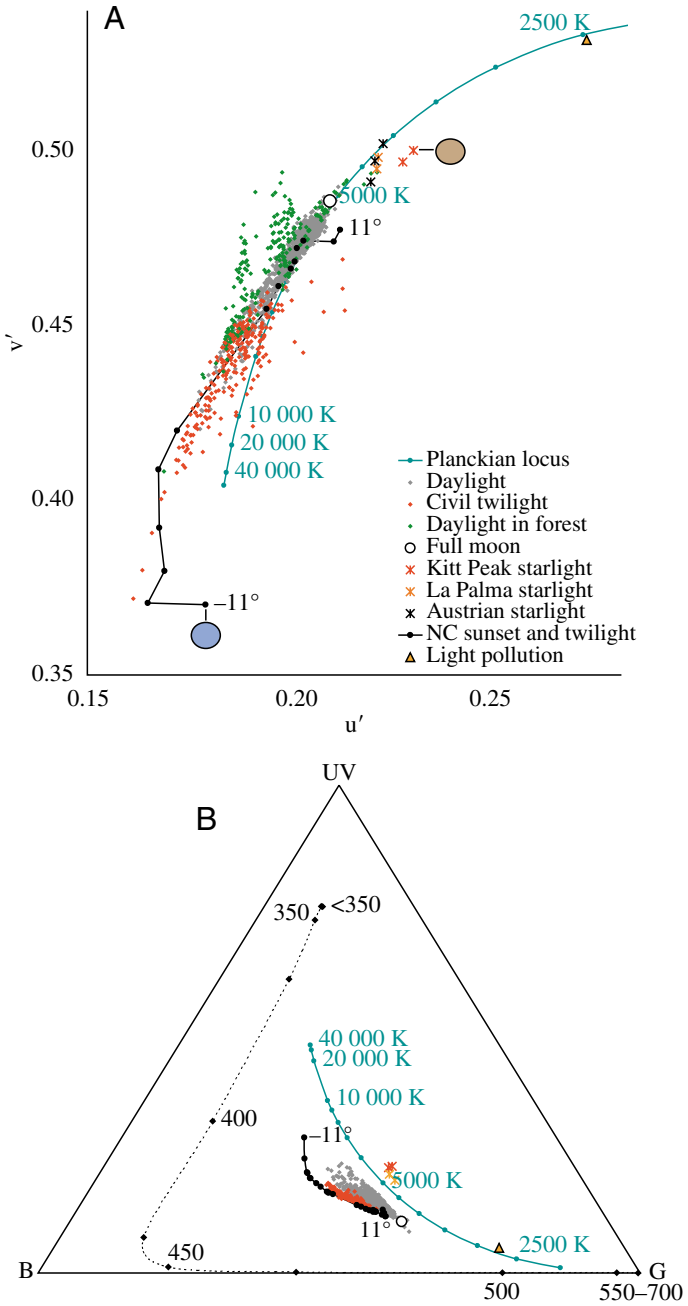

Fig. 3. (A) Human-based u′v′ chromaticities of daylight, sunset, twilight and nocturnal irradiances. The upper starlight symbols for the Kitt Peak and La Palma starlight data denote the chromaticities during a solar maximum; the lower symbols denote the chromaticities during a solar minimum. For comparison, the chromaticities of a 7° diameter patch of moonless sky (zenith angle 45°) under thin clouds, clear skies and overcast conditions are also shown (Höhn and Büchtermann, 1973). The black line denotes sunset and twilight data from North Carolina. Its symbols show data taken at solar elevation intervals of about 2°. The colored circles next to Kitt Peak starlight and '–11°' show the human-perceived colors at those two chromaticity extremes. The Planckian locus shows the chromaticities of blackbody radiators as a function of temperature. Data points for this locus are every 500 K up to 5000 K, and every 1000 K up to 10000 K, after which each point is labelled. (B) *Deilephila*-based relative quantum catches for the data shown in A. The three corners depict illuminants that are absorbed by one receptor only. The broken line shows the quantum catches of the spectral colors, with points every 25 nm and numbers every 50 nm. Because 49 of the civil twilight spectra and all 220 forest spectra were not taken at UV wavelengths, their relative quantum catches could not be calculated.

from 14% to 36% without color constancy and from 1% to 24% assuming von Kries color constancy (Fig. 5B–D). Unlike for the achromatic case, chromatic contrasts were higher for the blue and yellow flower than for the white flower and red wing.

Photon catches as a function of the λ_{max} of the long wavelength photoreceptor

Under nautical twilight, the photon catch of a receptor containing only one photopigment was relatively independent of the pigment's wavelength of peak absorption (λ_{max}), regardless of whether the stimulus was white, green or red (Fig. 6A–C). However, there was a gradual decrease for hypothetical receptors with λ_{max} at low visible and ultraviolet wavelengths. Under full moon and starlight though, the photon catch was strongly and positively correlated with λ_{max}, with catches of hypothetical photoreceptors with 650 nm pigments being 2–3 times greater than those for the actual 525 nm long wavelength photopigment. This correlation was particularly strong for photoreceptors viewing the red wings of *D. elpenor* (Fig. 6C). The source of nocturnal illumination (starlight or moonlight) had little effect on this correlation for all three stimuli.

In fused rhabdoms containing all three pigments, the variation of the relative quantum catches under the three illuminants (given by the area of the triangle formed by the three quantum catch loci) also increased with wavelength. At peak wavelengths greater than 600 nm, the variation was 50% greater than it was at 525 nm.

Discussion

Spectral range of crepuscular and nocturnal illumination

Crepuscular and nocturnal periods provide challenging visual environments, where variations in intensity of up to six orders of magnitude co-occur with significant spectral variation. As the solar elevation decreases from +20° to –20°, the downwelling irradiance is first relatively spectrally neutral, then long-wavelength dominated, then short-wavelength dominated, and then either spectrally neutral or long wavelength dominated depending on the presence or absence of the moon (i.e. white to red to blue and then back to white or red, as perceived by humans). The same pattern in opposite order occurs at sunrise, and although not measured due to the limited sensitivities of the spectrometers, it is safe to assume that the same pattern also occurs at moonrise and moonset (given that moonlight is reflected sunlight). At temperate and tropical latitudes, the rate of solar and lunar elevation change near the horizon is approximately 1° every 4–6 min

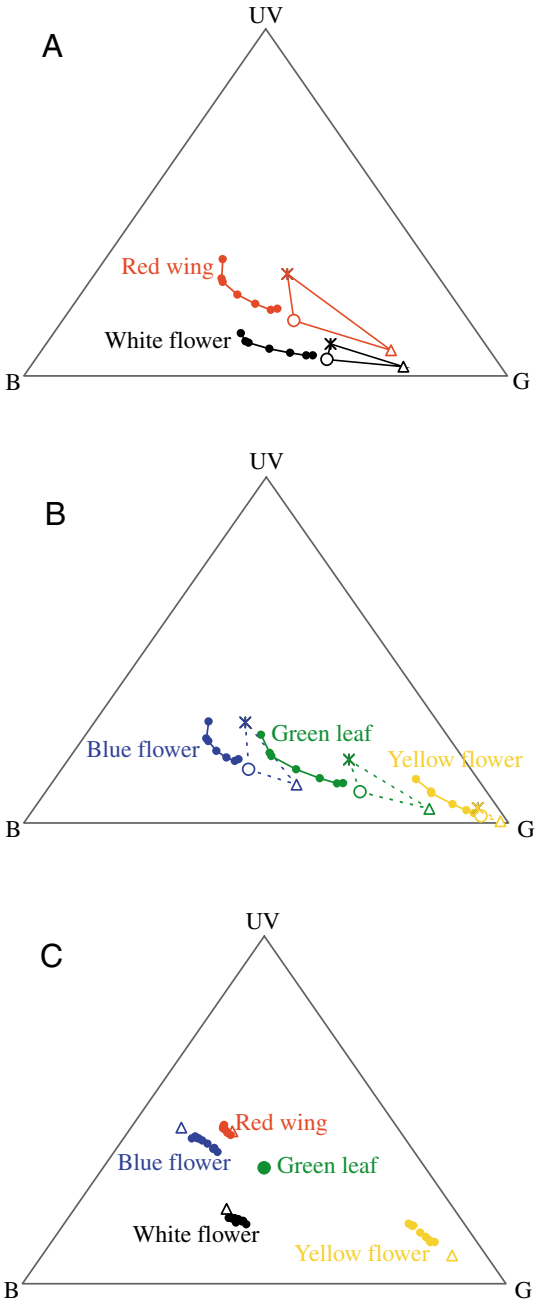

Fig. 4. (A,B) *Deilephila*-based relative quantum catches for the five different stimuli viewed under various sunset, twilight and nocturnal illuminants. Filled circles represent quantum catches of stimuli at sunset and twilight (solar elevation from 11° to –11°). Solar elevation decreases as data moves from right to left. Quantum catches under the nocturnal illuminants are to the right of those for sunset and twilight and consist of the following: open circles, quantum catches of stimuli under full moonlight; open triangles, quantum catches of stimuli under light polluted night sky; asterisks, quantum catches of stimuli under starlight only. (C) Quantum catches of the five stimuli assuming that *D. elpenor* has von Kries color constancy and is adapted to a background of green leaves under each illuminant (hence the central location of all the green stimuli). With the exception of light-polluted night skies (triangle), all the data have the same symbols for clarity.

(determined using US Naval Observatory tables). Thus, these intensity and spectral changes occur over a period of 2.5–4 h, with the central 20° range that exhibits the largest changes occurring in 80–120 min.

While cloud cover, solar elevation and the presence of a forest canopy also affect the spectral quality of daylight, the effect is smaller than what is observed during crepuscular periods and comparable to what is seen during the night. This is due partially to the fact that solar elevation has little effect on spectrum for elevations greater than 20°, and that clouds primarily scatter rather than absorb light, and thus have little effect on spectral quality. More important, however, is that the only two significant sources of daytime illumination are the sun and scattered sunlight, whose spectral characteristics and relative contributions both remain fairly constant at solar elevations greater than 20°. In contrast, crepuscular and nocturnal environments are lit by multiple sources with different spectra including a low-elevation sun or moon, high elevation moon, starlight, airglow emissions, and scattered sun or moonlight (Leinert et al., 1998). Because both the intensities and spatial extents of these sources vary by many orders of magnitude (Fig. 2C), spectral quality can change rapidly and significantly, particularly during the rising and setting of the sun or moon (Fig. 7). For example, near sunset the small, but intense and long-wavelength dominated solar disk balances the relatively dim short-wavelength dominated skylight until the sun nearly reaches the horizon, after which the general illumination changes rapidly from spectrally neutral to short-wavelength dominated.

Surprisingly, the intense blue of skylight during nautical twilight is not due to wavelength-dependent light scattering, but to absorption by ozone (Hulbert, 1953; Rozenberg, 1966). In addition to its strong absorption at ultraviolet wavelengths, ozone also has a broad absorption band in the visible, known as the Chappuis Band. While this absorption has only a minor effect on the spectrum of the daytime sky, it has a profound effect during late twilight. Without this absorption, which ranges from 450 to 700 nm and has double peaks at approximately 580 and 600 nm, skylight during nautical twilight would be a pale yellow (reviewed by Bohren, 2004). Because ozone concentration varies with season, geographic location and human activity (reviewed by Vingarzan, 2004), the spectra of skylight during nautical twilight are likely to be quite variable.

Changing crepuscular and nocturnal illumination and monochromatic visual systems

Although the exact achromatic contrasts depend on the spectral sensitivity of the viewer and the spectral reflectances of the targets and backgrounds, the examples given in this study show that they can vary significantly under the different crepuscular and nocturnal illuminants. With the exception of the white flower, the achromatic contrasts of the stimuli against the leaf background were quite variable. In certain cases, the contrast changed polarity. For example, the blue flower was brighter than the leaves during nautical twilight, but darker

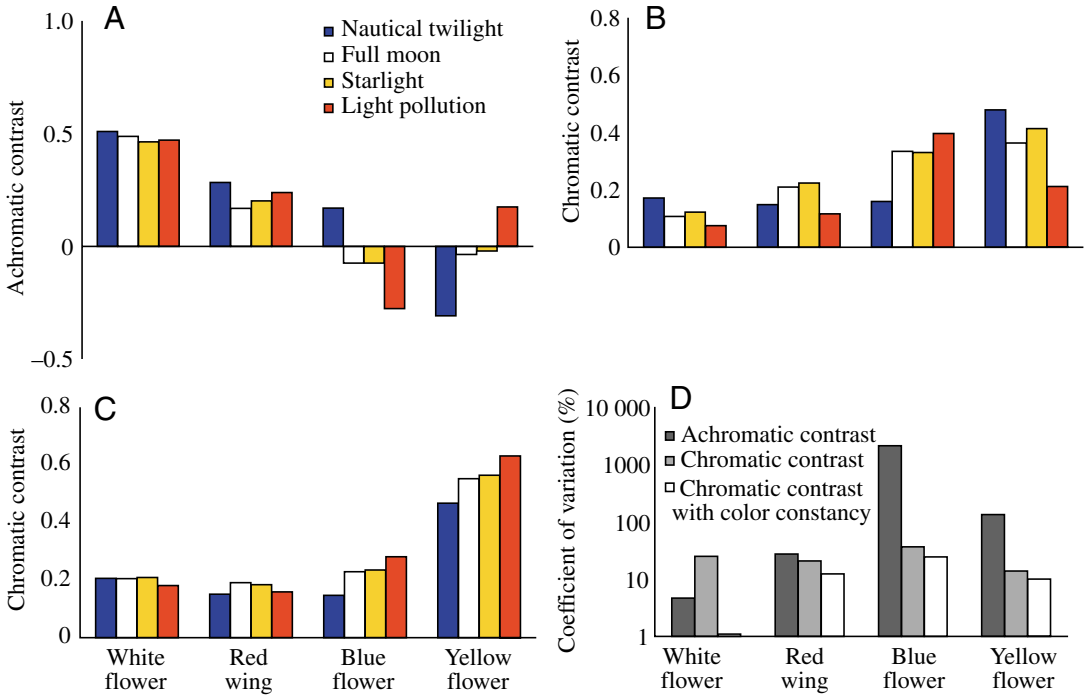

Fig. 5. (A) Achromatic contrast between four stimuli (the white evening primrose, the red hindwing of *D. elpenor*, the yellow flower, and the blue flower) and a green leaf background. Positive contrast indicates that the object is brighter than the background. (B) Chromatic contrast, defined as the distance between the relative quantum catches of the stimuli and the leaf background. (C) Chromatic contrast assuming that *D. elpenor* has von Kries color constancy and is adapted to a background of green leaves under each illuminant. (D) Coefficients of variation of the achromatic and chromatic contrasts of the four stimuli when viewed under nautical twilight, moonlight and starlight.

than the leaves during night. In addition, two of the stimuli (the blue and yellow flowers) had low contrasts under moonlight and starlight, likely rendering them undetectable *via* achromatic cues.

In contrast, the white flower, whose reflectance is high but relatively similar in spectrum to the leaves, had a high and stable contrast under all light conditions (Fig. 5A). *D. elpenor* and other nocturnal hawkmoths are thought to primarily visit white flowers with exceptionally high reflectance (reviewed by Raguso and Willis, 2002; Kelber et al., 2003a). In addition, crepuscular hawkmoths (e.g. *Manduca sexta*), and those that are active both during day and night (e.g. *Hyles* sp.), tend to visit blue and yellow flowers in bright light but white flowers in dim light (reviewed by Raguso and Willis, 2002).

The need for stability of achromatic contrast may also explain why the nocturnal flowers of many bat-pollinated species tend to be red or white. Flower-visiting bats are color-blind at night (Winter et al., 2003) and thus rely on achromatic contrast. Because the illumination during moonlit and starlit nights is long-wavelength shifted, red flowers are bright relative to green leaves, resulting in a high and more stable contrast. However, because the peak wavelength of the long-wavelength pigments of some of these bats is relatively low (~510 nm), they may not be able to exploit this contrast.

In general, however, achromatic contrast depends strongly on the illuminant, which varies significantly during crepuscular and nocturnal periods. This variation, which occurs whenever spectrally different stimuli and backgrounds are viewed under highly variable illuminants, makes monochromatic vision unreliable during these periods.

Chromatic contrasts and color constancy

While chromatic contrasts varied less than achromatic contrasts (Fig. 5D), the addition of color constancy, which has recently been demonstrated for *D. elpenor* (Balkenius and Kelber, 2004), reduces the variation further. Chromatic contrasts without constancy are affected by the fact that the different lighting conditions changed the relative quantum catches from different colored stimuli in different ways. For example, relative quantum catches from the yellow flower *Lotus corniculatus* viewed under moonlight and nautical twilight changed less than did the relative quantum catches from the green leaf background (Fig. 4B). This is due to the fact that the relative contribution of the long-wavelength light that the yellow flower reflects changes less than the relative contribution of the middle wavelength light that the leaf reflects (Figs 1A, 2A,B). The result is not only a shift in the color of the scene, but also of the chromatic contrast between the flower and the leaf background. Color constancy, which can be explained as the result of receptor adaptation, reduces the variation for all four stimuli. In the case of the white flower, whose variation in chromatic contrast is greater than its variation in achromatic contrast, color constancy removes nearly all the variation.

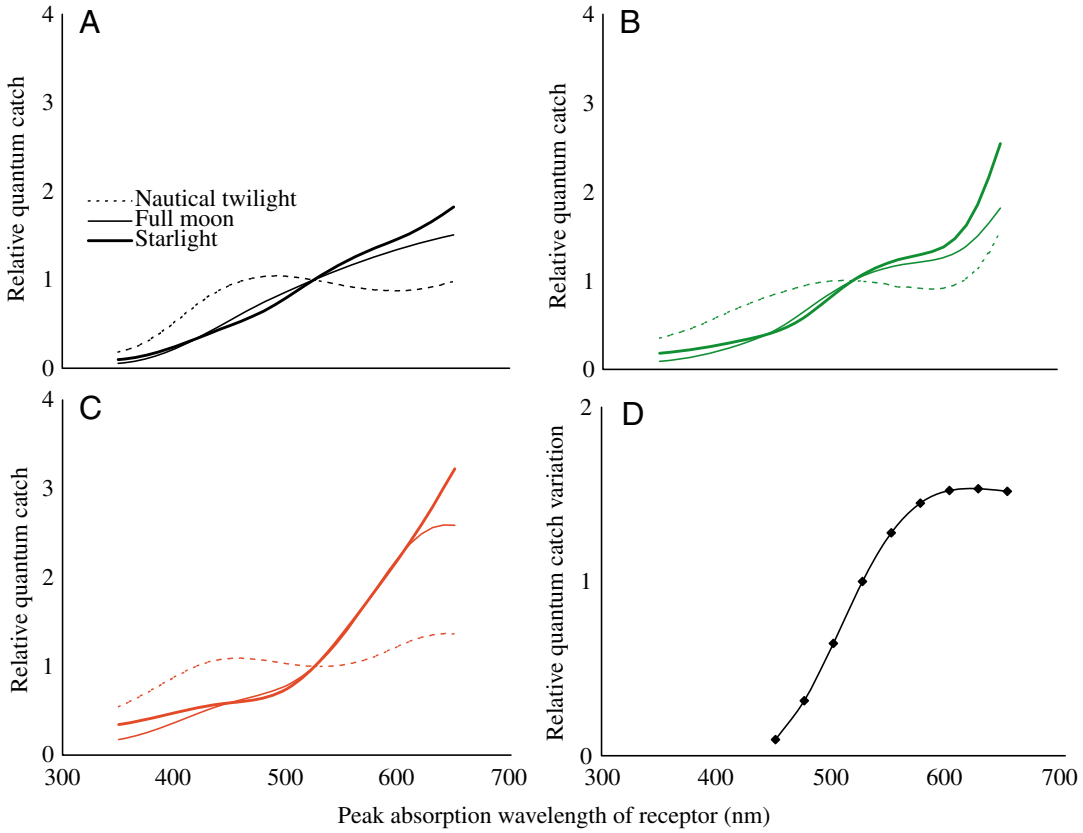

Fig. 6. (A–C) Numbers of photons absorbed by a hypothetical photoreceptor with a given λ_{max} relative to the number absorbed by the green receptor possessed by *D. elpenor* (λ_{max}=525 nm) under three illuminants (nautical twilight, full moon, starlight). (A) Viewing the white evening primrose. (B) Viewing green leaves. (C) Viewing the red hindwing of a conspecific. (D) The variation in relative quantum catches (among nautical twilight, moonlight and starlight), in a fused rhabdom containing all three visual pigments, as a function of the wavelength of the long wavelength receptor. The variation is estimated by the area of the triangle formed by the three points in the Maxwell triangle. As in A–C, the variation at 525 nm is set to 1.

The function of nocturnal color vision in *D. elpenor* is poorly understood. As mentioned above, nocturnal hawkmoths are thought to visit white flowers at night, which can reliably be detected without color vision. However, given that other hawkmoths visit blue and yellow flowers during the day, it is possible that flowers of these colors are also visited at night. Given their unreliable appearance to monochromatic visual systems, blue and yellow flowers may remain undetected by competitors of *D. elpenor*, allowing them to exploit an additional source of nectar.

The general long-wavelength shift of nocturnal illumination and the red coloration of *D. elpenor* render this species quite visible at night. Also, it has relatively stable achromatic and chromatic contrasts (Fig. 5). While many hawkmoths have some red coloration, particularly on their hindwings (which is thought to function as a startle display), the more extensive red coloration of *D. elpenor* is less common (Kitching and Cadiou, 2000). This raises

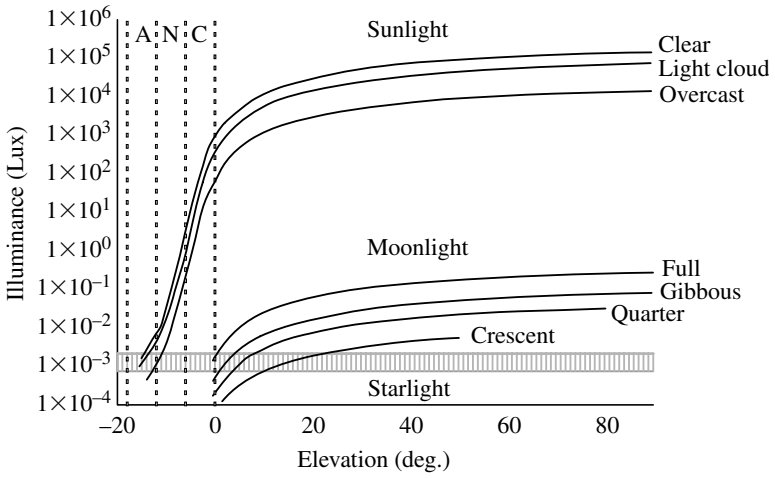

Fig. 7. The variation of sunlight and moonlight relative to starlight as a function of the elevation of the sun or moon, the sky conditions, and the phase of the moon. A, N and C refer to astronomical, nautical and civil twilight, respectively. (Modified from Bond and Henderson, 1963.)

the possibility that color vision may enhance recognition of conspecifics or be used in mating. While mating in moths is thought to be entirely mediated by olfaction, most tasks are eventually found to involve multiple sensory modalities. For example, nocturnal foraging in hawkmoths is known to involve both visual and olfactory cues (Raguso and Willis, 2002).

Absolute numbers of captured photons as a function of λ_{max}

While the relationship between visual pigment maxima and illuminant spectra under diurnal conditions is complex, research on deep-sea fish has shown that, at least in that particular light-limited environment, visual sensitivity peaks close to the wavelength of peak illumination (reviewed by Partridge and Cummings, 1999). This characteristic, which maximizes photon catch, does not appear to operate in *D. elpenor*. The peak wavelength is similar to those found in the long wavelength receptors of diurnal moths (Briscoe and Chittka, 2001), and differs substantially from that leading to maximal photon catch (Fig. 6A–C). This is intriguing, given the extreme light limitation present during color vision under starlight (Kelber et al., 2002), and the presence of longer wavelength pigments in the Lepidoptera (Briscoe and Chittka, 2001). In vertebrates, the higher noise levels in long-wavelength ciliary receptors (dark noise) (Barlow, 1957; Donner et al., 1990; Firsov and Govardovskii, 1990; Ala-Laurila et al., 2004) may account for this. However, dark noise appears to play a minor role in invertebrates due to different transduction mechanisms in rhabdomeric receptors (Laughlin, 1990; Warrant, 2004). Because relative quantum catches in the fused rhabdoms of *D. elpenor* vary more with changing illuminant as the peak wavelength of the long-wavelength receptor increases (Fig. 6C), the 525 nm peak may be a compromise between sensitivity and color stability. The peak wavelengths of the photoreceptors may also be constrained by their function during diurnal periods.

It is also possible that the sub-optimal λ_{max} of the long wavelength pigment is due to a phylogenetic or other constraint. Indeed, a survey of visual pigment maxima in insects by Briscoe and Chittka (2001) found little correlation with environment or behavior. However, at least two nocturnal species in the moth family Noctuidae have a fourth visual pigment (λ_{max}=560, 580 nm) (Langer et al., 1979; Ichikawa and Tateda, 1982), which phylogenetic analyses suggest are independently evolved within the Lepidoptera (Briscoe and Chittka, 2001). The function of these pigments at nocturnal light levels is doubtful given the limited optical sensitivity of noctuid eyes (A. Kelber, unpublished data), but their existence casts some doubt on a phylogenetic constraints argument.

Light pollution

Anthropogenic light sources (‘light pollution’) are an increasingly dominant factor in nocturnal illumination (e.g. Cinzano et al., 2001; Garstang, 2004). In addition to reaching intensities comparable to the light during nautical twilight or under the full moon, spectral irradiance under light polluted skies is substantially different from that found under any natural illumination (Fig. 3). While light pollution spectra have many peaks (primarily due to mercury and sodium emission lamps), the primary spectral difference is a large increase in the relative contribution of long-wavelength light. This significantly changed both the achromatic and chromatic contrasts of the considered stimuli. The achromatic contrasts of the blue and yellow flowers in particular were significantly altered.

Light pollution can rival the intensity of the blue sky during nautical twilight and essentially has an opposite spectrum: the former being strongly long-wavelength shifted, the latter strongly short-wavelength shifted. Therefore the color of twilight illumination in urban and other light-polluted regions will vary rapidly over an unnaturally large range, potentially presenting significant difficulties for both monochromatic and color-visual species operating during this period.

Recent research on the ecological effects of light pollution (reviewed by Longcore and Rich, 2004) has generally focused on its intensity. To our knowledge, however, no studies have examined the effect of the color of light pollution. Given its unusual spectrum, it may have a significant effect on the foraging and mating of crepuscular and nocturnal species.

Conclusions

The spectral quality of crepuscular and nocturnal illumination varies over a larger range than does that of diurnal illumination, even when a wide range of atmospheric and forest conditions are considered. This variation makes monochromatic visual systems unreliable during these periods. We propose, for species that forage during twilight and night, that the increased signal reliability afforded by color constant color vision offsets the decreased sensitivity and provides an explanation for this unusual trait. However, the preference of *D. elpenor* for white flowers, which have stable achromatic contrasts, complicate the picture for this species. The mismatch of the long-wavelength pigment to the spectra of nocturnal illumination results in a less than optimal photon catch, but may lead to higher color stability. Light polluted night skies are strongly long-wavelength shifted and substantially alter the appearance of objects. Future research into nocturnal vision will need to consider the large natural and anthropogenic variability of this optical environment.

Appendix

Calculation of relative quantum catches assuming a fused rhabdom containing equal volumes and cross-sectional areas for each photopigment

$L(\lambda)$ is the stimulus strength (in quanta) at distal surface of the rhabdom; $R_i(\lambda)$ is the absorbance curve of ith pigment, where i=UV, B or G, normalized to a peak of 1; $\bar{R}(\lambda)$ is the un-normalized average of the three absorbance curves; and k and l are absorption coefficient and length of the rhabdom, respectively.

The number of photons of wavelength λ that penetrate a distance x into the rhabdom equals:

$$L(\lambda)e^{-k\bar{R}(\lambda)x} . \quad \text{(A1)}$$

The fraction of these photons that are absorbed by a dx thick section of the portion of the rhabdom containing the ith photopigment equals:

$$\frac{1 - e^{-kR_i(\lambda)dx}}{3} \cong \frac{kR_i(\lambda)}{3} dx \quad \text{(A2)}$$

(from Taylor expansion of e^x for small x).

Thus, the total number of photons absorbed by the ith photopigment at wavelength λ by the entire rhabdom equals:

$$Q_i(\lambda) = \frac{1}{3} L(\lambda) kR_i(\lambda) \int_0^l e^{-k\bar{R}(\lambda)x} dx = \left| -\frac{1}{3} L(\lambda) \frac{kR_i(\lambda)}{k\bar{R}(\lambda)} e^{-k\bar{R}(\lambda)x} \right|_0^l . \quad \text{(A3)}$$

Evaluating this integral at l and 0 gives:

$$Q_i(\lambda) = -\frac{1}{3} L(\lambda) \frac{R_i(\lambda)}{\bar{R}(\lambda)} e^{-k\bar{R}(\lambda)l} + \frac{1}{3} L(\lambda) \frac{R_i(\lambda)}{\bar{R}(\lambda)} = \frac{1}{3} L(\lambda) \frac{R_i(\lambda)}{\bar{R}(\lambda)} (1 - e^{-k\bar{R}(\lambda)l}) . \quad \text{(A4)}$$

Therefore, the total quantum catch by the ith photopigment is:

$$Q_i = \frac{1}{3} \sum_{\lambda=300\ nm}^{\lambda=700\ nm} L(\lambda) \frac{R_i(\lambda)}{\bar{R}(\lambda)} (1 - e^{-k\bar{R}(\lambda)l}) \Delta\lambda . \quad \text{(A5)}$$

The color locus of a given stimulus $L(\lambda)$ is (X_1,X_2), where:

$$X_1 = \frac{1}{\sqrt{2}} (q_G - q_B) , \quad \text{and} \quad X_2 = \frac{\sqrt{2}}{\sqrt{3}} \left(q_{UV} - \frac{q_G + q_B}{2} \right) , \quad \text{(A6)}$$

where:

$$q_{UV} = \frac{Q_{UV}}{Q_{UV} + Q_B + Q_G} , \quad q_B = \frac{Q_B}{Q_{UV} + Q_B + Q_G} , \quad q_G = \frac{Q_G}{Q_{UV} + Q_B + Q_G} . \quad \text{(A7)}$$

Before the calculation of the relative quantum catches, the Q_i values are normalized so that $Q_{uv}=Q_B=Q_G$ for any spectrally neutral (e.g. color-less) stimulus. This maps these stimuli to the center of the color triangle. This normalization is done by dividing each Q_i by

$$\sum_{\lambda=300\ nm}^{\lambda=700\ nm} \frac{R_i(\lambda)}{\bar{R}(\lambda)} (1 - e^{-k\bar{R}(\lambda)l}) . \quad \text{(A8)}$$

The authors thank Dr C. C. Chiao for providing forest spectra, Dr Marianne Moore for providing urban night spectra, and Drs Philip Massey and Christopher Benn for providing starlight spectra. S.J. and A.S. were supported in part by a grant from the National Science Foundation (IOB-0444674). A.K. and E.J.W. are grateful for the ongoing support of the Swedish Research Council. R.L. was supported by United States National Science Foundation grant ATM-0207516 and by the United States Naval Academy's Departments of Physics and Mathematics. J.H.-A. was supported by Spain's Comisión Interministerial de Ciencia y Tecnología (CICYT) under research grant DPI2004-03734. This is contribution number 1618 of the Harbor Branch Oceanographic Institution.

References

Ala-Laurila, P., Donner, K. and Koskelainen, A. (2004). Thermal activation and photoactivation of visual pigments. *Biophys. J.* **86**, 3653-3662.

Balkenius, A. and Kelber, A. (2004). Colour constancy in diurnal and nocturnal hawkmoths. *J. Exp. Biol.* **207**, 3307-3316.

Barlow, H. B. (1957). Purkinje shift and retinal noise. *Nature* **179**, 255-256.

Benn, C. R. and Ellison, S. (1998). La Palma night-sky brightness. *New Astron. Rev.***42**, 503-527.

Bohren, C. F. (2004). Atmospheric optics. In *The Optics Encyclopedia* (ed. T. G. Brown), pp. 53-91. New York: Wiley-VCH.

Bond, D. S. and Henderson, F. P. (1963). *The Conquest of Darkness. (AD 346297).* Alexandria: Defense Documentation Center.

Briscoe, A. D. and Chittka, L. (2001). The evolution of color vision in insects. *Ann. Rev. Entomol.* **46**, 471-510.

Chiao, C. C., Osorio, D., Vorobyev, M. and Cronin, T. W. (2000). Characterization of natural illuminants in forests and the use of digital video data to reconstruct illuminant spectra. *J. Opt. Soc. Am. A* **17**, 1713-1721.

Chittka, L., Shmida, A., Troje, N. and Menzel, R. (1994). Ultraviolet as a component of flower reflections, and the colour perception of Hymenoptera. *Vision Res.* **34**, 1489-1508.

Cinzano, P., Falchi, F. and Elvidge, C. D. (2001). The first world atlas of the artificial night sky brightness. *Month Not. R. Astron. Soc.* **328**, 689-707.

Cronin, T. W. and Frank, T. M. (1996). A short-wavelength photoreceptor class in a deep-sea shrimp. *Proc. R. Soc. Lond. B* **263**, 861-865.

Donner, K., Firsov, M. L. and Govardovskii, V. I. (1990). The frequency of isomerization-like 'dark' events in rhodopsin and porphyropsin rods of the bull-frog retina. *J. Physiol. (Lond.)* **428**, 673-692.

Douglas, R. H., Partridge, J. C. and Marshall, N. J. (1998). The eyes of deep sea fish. I. Lens pigmentation, tapeta and visual pigments. *Prog. Retin. Eye Res.* **17**, 597-636.

Doxaran, D., Cherukuru, N. C., Lavender, S. J. and Moore, G. F. (2004). Use of a spectralon panel to measure the downwelling irradiance signal: case studies and recommendations. *Appl. Opt.* **43**, 5981-5986.

Endler, J. A. (1991). Variations in the appearance of guppy color patterns to guppies and their predators under different visual conditions. *Vision Res.* **31**, 587-608.

Firsov, M. L. and Govardovskii, V. I. (1990). Dark noise of visual pigments with different absorption maxima. *Sensornye Sistemy* **4**, 25-34.

Garstang, R. H. (2004). Mount Wilson Observatory: The sad story of light pollution. *Observatory* **124**, 14-21.

Hernández-Andrés, J., Romero, J., Nieves, J. L. and Lee, R. L., Jr (2001). Color and spectral analysis of daylight in southern Europe. *J. Opt. Soc. Am. A* **18**, 1325-1335.

Höglund, G., Hamdorf, K. and Rosner, G. (1973). Trichromatic visual system in an insect and its sensitivity control by blue light. *J. Comp. Physiol. A* **86**, 265-279.

Höhn, D. H. and Büchtermann, W. (1973). Spectral radiance in the S20-range and luminance of the clear and overcast night sky. *Appl. Opt.* **12**, 52-61.

Hulbert, O. (1953). Explanation of the brightness and color of the sky, particularly the twilight sky. *J. Opt. Soc. Am. A* **43**, 113-118.

Ichikawa, T. and Tateda, H. (1982). Distribution of color receptors in the

larval eyes of fours species of lepidoptera. *J. Comp. Physiol. A* **149**, 317-324.

Jacobs, G. H. (1993). The distribution and nature of colour vision among the mammals. *Biol. Rev.* **68**, 413-471.

Johnsen, S. and Sosik, H. M. (2003). Cryptic coloration and mirrored sides as camouflage strategies in near-surface pelagic habitats: implications for foraging and predator avoidance. *Limnol. Oceanogr.* **48**, 1277-1288.

Kelber, A., Balkenius, A. and Warrant, E. J. (2002). Scotopic colour vision in nocturnal hawkmoths. *Nature* **419**, 922-925.

Kelber, A., Balkenius, A. and Warrant, E. J. (2003a). Colour vision in diurnal and nocturnal hawkmoths. *Integr. Comp. Biol.* **43**, 571-579.

Kelber, A., Vorobyev, M. and Osorio, D. (2003b). Colour vision in animals – behavioural tests and physiological concepts. *Biol. Rev.* **78**, 81-118.

Kitching, I. J. and Cadiou, J.-M. (2000). *Hawkmoths of the World: An Annotated and Illustrated Revisionary Checklist (Lepidoptera: Sphingidae).* New York: Cornell University Press.

Langer, H., Haumann, B. and Meinecke, C. C. (1979). Tetrachromatic visual system in the moth *Spodoptera exempta* (Insecta: Noctuidae). *J. Comp. Physiol. A* **129**, 235-239.

Laughlin, S. B. (1990). Invertebrate vision at low luminances. In *Night Vision* (ed. R. F. Hess, L. T. Sharpe and K. Nordby), pp. 223-250. Cambridge: Cambridge University Press.

Laughlin, S. B. and Hardie, R. C. (1978). Common strategies for light adaptation in the peripheral visual systems of fly and dragonfly. *J. Comp. Physiol. A* **128**, 319-340.

Lee, R. L., Jr and Hernández-Andrés, J. (2003). Measuring and modeling twilight's purple light. *Appl. Opt.* **42**, 445-457.

Leinert, C., Bowyer, S., Haikala, L. K., Hanner, M. S., Hauser, M. G., Levasseur-Regourd, A.-Ch., Mann, I., Mattila, K., Reach, W. T., Schlosser, W. et al. (1998). The 1997 reference of diffuse night sky brightness. *Astron. Astrophys. Ser.* **127**, S1-S99.

Longcore, T. and Rich, C. (2004). Ecological light pollution. *Front. Ecol. Environ.* **2**, 191-198.

Lovell, P. G., Tolhurst, D. J., Parraga, C. A., Baddeley, R., Leonards, U., Troscianko, J. and Troscianko, T. (2005). Stability of the color opponent signals under changes of illuminant in natural scenes. *J. Opt. Soc. Am. A* **22**, 2060-2071.

Makino-Tasaka, M. and Suzuki, T. (1984). The green rod pigment of the bullfrog, *Rana catesbeiana*. *Vision Res.* **24**, 309-322.

Massey, P. and Foltz, C. B. (2000). The spectrum of the night sky over Mount Hopkins and Kitt Peak: changes after a decade. *Pub. Astron. Soc. Pacif.* **112**, 566-573.

Mattila, K. (1980). Synthetic spectrum of the integrated starlight between 3000 and 10000 Å. Part 1. Method of calculation and results. *Astron. Astrophys. Ser.* **39**, S53-S65.

McFarland, W. N., Wahl, C., Suchanek, T. and McAlary, F. (1999). The behavior of animals around twilight with emphasis on coral reef communities. In *Adaptive Mechanisms in the Ecology of Vision* (ed. S. N. Archer, M. B. A. Djamgoz, E. R. Loew, J. C. Partridge and S. Vallerga), pp. 583-628. Boston: Kluwer Academic.

Munz, F. W. and McFarland, W. N. (1977). Evolutionary adaptations of fishes to the photic environment. In *The Visual System of Vertebrates* (ed. F. Crescitelli), pp. 194-274. New York: Springer-Verlag.

Palmer, J. M. (1995). The measurement of transmission, absorption, emission, and reflection. In *Handbook of Optics II* (ed. M. Bass, E. W. Van Strylan, D. R. Williams and W. L. Wolfe), pp. 25.1-25.25. New York: McGraw-Hill Inc.

Partridge, J. C. and Cummings, M. E. (1999). In *Adaptive Mechanisms in the Ecology of Vision* (ed. S. N. Archer, M. B. A. Djamgoz, E. R. Loew, J. C. Partridge and S. Vallerga), pp. 251-284. Boston: Kluwer Academic.

Raguso, R. A. and Willis, M. A. (2002). Synergy between visual and olfactory cues in nectar feeding by naive hawkmoths, *Manduca sexta*. *Anim. Behav.* **64**, 685-695.

Rickel, S. and Genin, A. (2005). Twilight transitions in coral reef fish: the input of light induced changes in foraging behavior. *Anim. Behav.* **70**, 133-144.

Roth, L. S. V. and Kelber, A. (2004). Nocturnal colour vision in geckos. *Proc. R. Soc. Lond. B* **6**, S485-S487.

Rozenberg, G. V. (1966). *Twilight: A Study in Atmospheric Optics.* New York: Plenum Press.

Schwemer, J. and Paulsen, R. (1973). Three visual pigments in *Deilephila elpenor* (Lepidoptera, Sphingidae). *J. Comp. Physiol. A* **86**, 215-229.

Snyder, A. W., Menzel, R. and Laughlin, S. B. (1973). Structure and function of the fused rhabdom. *J. Comp. Physiol. A* **87**, 99-135.

Stavenga, D. G., Smits, R. P. and Hoenders, B. J. (1993). Simple exponential functions describing the absorbance bands of visual pigment spectra. *Vision Res.* **33**, 1011-1017.

Vingarzan, R. (2004). A review of surface ozone background levels and trends. *Atmos. Environ.* **38**, 3431-3442.

von Kries, J. (1904). Die Gesichtsempfindungen. In *Handbuch der Physiologie des Menschen*, *Vol. 3* (ed. W. Nagel), pp. 109-282. Braunschweig: Vieweg.

Warrant, E. J. (2004). Vision in the dimmest habitats on earth. *J. Comp. Physiol. A* **190**, 765-789.

Warrant, E. J. and Nilsson, D.-E. (1998). Absorption of white light in photoreceptors. *Vision Res.* **38**, 195-207.

Winter, Y., López, J. and von Helversen, O. (2003). Ultraviolet vision in a bat. *Nature* **425**, 612-614.

Wyszecki, G. and Stiles, W. S. (1982). *Color Science: Concepts and Methods, Quantitative Data and Formulae*. New York: John Wiley and Sons.